Mon. Not. R. Astron. Soc. **419,** 2077–2088 (2012) doi:10.1111/j.1365-2966.2011.19859.x

Asteroseismology of old open clusters with *Kepler:* direct estimate of the integrated red giant branch mass-loss in NGC 6791 and 6819

A. Miglio,[1⋆] K. Brogaard,[2] D. Stello,[3] W. J. Chaplin,[1] F. D'Antona,[4] J. Montalbán,[5] S. Basu,[6] A. Bressan,[7,8] F. Grundahl,[9] M. Pinsonneault,[10] A. M. Serenelli,[11] Y. Elsworth,[1] S. Hekker,[1,12] T. Kallinger,[13] B. Mosser,[14] P. Ventura,[4] A. Bonanno,[15] A. Noels,[5] V. Silva Aguirre,[16] R. Szabo,[17] J. Li,[18] S. McCauliff,[19] C. K. Middour[19] and H. Kjeldsen[9]

[1]*School of Physics and Astronomy, University of Birmingham, Edgbaston, Birmingham B15 2TT*
[2]*Department of Physics and Astronomy, University of Victoria, PO Box 3055, Victoria, BC V8W 3P6, Canada*
[3]*Sydney Institute for Astronomy (SIfA), School of Physics, University of Sydney, NSW 2006, Australia*
[4]*INAF - Osservatorio Astronomico di Roma, via Frascati 33, Monteporzio Catone (RM), Italy*
[5]*Institut d'Astrophysique et de Géophysique de l'Université de Liège, Allée du 6 Août, 17 B-4000 Liège, Belgium*
[6]*Department of Astronomy, Yale University, PO Box 208101, New Haven, CT 06520-8101, USA*
[7]*SISSA, via Bonomea 265, 34136 Trieste, Italy*
[8]*INAF - Osservatorio Astronomico di Padova, Vicolo dell'Osservatorio 5, I-35122 Padova, Italy*
[9]*Department of Physics and Astronomy, Building 1520, Aarhus University, 8000 Aarhus C, Denmark*
[10]*Department of Astronomy, Ohio State University, 140 West 18th Avenue, Columbus, OH 43210, USA*
[11]*Institute for Space Sciences (CSIC-IEEC), Facultad de Ciencies, Campus UAB, 08193 Bellaterra, Spain*
[12]*Astronomical Institute Anton Pannekoek, University of Amsterdam, Science Park 904, 1098 XH Amsterdam, the Netherlands*
[13]*Department of Physics and Astronomy, University of British Colombia, 6224 Agricultural Road, Vancouver, BC V6T 1Z1, Canada*
[14]*LESIA, CNRS, Université Pierre et Marie Curie, Université Denis Diderot, Observatoire de Paris, 92195 Meudon Cedex, France*
[15]*INAF - Osservatorio Astrofisico di Catania, Via S.Sofia 78, 95123 Catania, Italy*
[16]*Max Planck Institute for Astrophysics, Karl-Schwarzschild-Str. 1, 85748 Garching bei München, Germany*
[17]*Konkoly Observatory of the Hungarian Academy of Sciences, Konkoly Thege Miklós út 15-17, H-1121 Budapest, Hungary*
[18]*SETI Institute/NASA Ames Research Center, Moffett Field, CA 94035, USA*
[19]*Orbital Sciences Corporation/NASA Ames Research Center, Moffett Field, CA 94035, USA*

Accepted 2011 September 20. Received 2011 September 14; in original form 2011 August 12

ABSTRACT

Mass-loss of red giant branch (RGB) stars is still poorly determined, despite its crucial role in the chemical enrichment of galaxies. Thanks to the recent detection of solar-like oscillations in G–K giants in open clusters with *Kepler*, we can now directly determine stellar masses for a statistically significant sample of stars in the old open clusters NGC 6791 and 6819. The aim of this work is to constrain the integrated RGB mass-loss by comparing the average mass of stars in the red clump (RC) with that of stars in the low-luminosity portion of the RGB [i.e. stars with $L \lesssim L(\mathrm{RC})$]. Stellar masses were determined by combining the available seismic parameters $\nu_{\max}$ and $\Delta\nu$ with additional photometric constraints and with independent distance estimates. We measured the masses of 40 stars on the RGB and 19 in the RC of the old metal-rich cluster NGC 6791. We find that the difference between the average mass of RGB and RC stars is small, but significant [$\Delta\overline{M} = 0.09 \pm 0.03$ (random) ± 0.04 (systematic) $\mathrm{M}_{\odot}$]. Interestingly, such a small $\Delta\overline{M}$ does not support scenarios of an extreme mass-loss for this metal-rich cluster. If we describe the mass-loss rate with Reimers prescription, a first comparison with isochrones suggests that the observed $\Delta\overline{M}$ is compatible with a mass-loss efficiency parameter in the range $0.1 \lesssim \eta \lesssim 0.3$. Less stringent constraints on the RGB mass-loss rate are set by the analysis of the ∼2 Gyr old NGC 6819, largely due to the lower mass-loss

⋆E-mail: miglioa@bison.ph.bham.ac.uk

expected for this cluster, and to the lack of an independent and accurate distance determination. In the near future, additional constraints from frequencies of individual pulsation modes and spectroscopic effective temperatures will allow further stringent tests of the $\Delta\nu$ and $\nu_{\rm max}$ scaling relations, which provide a novel, and potentially very accurate, means of determining stellar radii and masses.

Key words: asteroseismology – stars: late-type – stars: mass-loss – open clusters and associations: individual: NGC 6791 – open clusters and associations: individual: NGC 6819.

1 INTRODUCTION

The mass-loss rates of evolved stars are of primary importance for stellar and galactic evolution models, but neither the theory nor the observations are adequate to place reliable direct quantitative constraints. The mass-loss from asymptotic giant branch (AGB) stars is reasonably well understood in terms of global pulsations lifting gas out to distances above the photosphere where dust forms (e.g. Wood 1979; Bowen 1988), and the action of radiation pressure on the dust that further drives dust and gas away (e.g. Höfner 2009, and references therein). In contrast, there is no reliable theory for the mass-loss of cool, dust-free red giants, and even the wind acceleration mechanism remains unknown for the red giant branch (RGB). For these stars, no known mechanisms can yet satisfactorily explain the observed wind characteristics (for further discussion, see Lafon & Berruyer 1991; Harper 1996).

Indirect information is, however, available on the integrated mass-loss on the first giant branch (see e.g. Catelan 2009, for a recent review). This is important because it may involve a substantial amount of mass, especially for the lower mass stars undergoing the helium core flash, and thus may affect the initial to final mass relation and the amount of mass recycled into the interstellar medium. In the case of globular cluster (GC) stars, mass-loss along the RGB, and its spread, affects the distribution of stars along the horizontal branch (HB). This is because the morphology of the core-helium-burning track depends on the ratio between the helium core mass and the hydrogen-rich envelope mass, or, in other words, on the relative roles played by the core-helium-burning and the hydrogen shell burning (e.g. Sweigart & Gross 1976). The indirect evidence tells us that in GCs more mass is lost on the RGB than the AGB, since the typical stellar mass on the HB is $\sim$0.6 $\mathrm{M}_{\odot}$, with turn-off masses of $\sim$0.8 $\mathrm{M}_{\odot}$, and white dwarfs masses of $\sim$0.5–0.55 $\mathrm{M}_{\odot}$ (Kalirai et al. 2009).

The standard picture that the mass distribution along the HB matches mass-loss on the RGB has been questioned in the last decade. The ubiquitous presence of multiple populations in GCs has now become evident (e.g. Gratton et al. 2001; Piotto et al. 2007; Carretta et al. 2009), and the proposal that the stellar helium content of the different populations also has a role in determining the HB morphology (D'Antona et al. 2002; D'Antona & Caloi 2004) was confirmed by the presence of multiple main sequences in some GCs (Piotto et al. 2005, 2007).

In order to describe the mass-loss along the RGB, researchers rely on empirical laws like that of Reimers (1975a,b) which is based on observations of Population I giants, and which describes mass-loss rates as a function of stellar luminosity, radius and surface gravity. While subsequent work (Mullan 1978; Goldberg 1979; Judge & Stencel 1991; Catelan 2000; Schröder & Cuntz 2007) led to slight refinements, a variant of the 'Reimers law' is generally used to compute stellar evolution models of cool stars at all ages and metallicities.

Several observational indications on the RGB mass-loss have emerged in recent years. Origlia et al. (2002) detected the circumstellar matter around GC red giants using the ISOCAM camera onboard the *ISO* satellite, and derived mass-loss rates for a few RGB stars. A first empirical mass-loss law was proposed by Origlia et al. (2007), based on the observations by IRAC, onboard *Spitzer*, of the GC 47 Tuc. They found mass-loss to be episodic, depending less on luminosity than in Reimers law, and occurring predominantly in the upper $\sim$2 mag of the RGB (Origlia et al. 2010). These findings were questioned by Boyer et al. (2010) and McDonald et al. (2011a,b), who found no evidence for dust production in stars with $L < 1000\,\mathrm{L}_{\odot}$. By comparing with HB models, they showed that mass-loss on the RGB of 47 Tuc is likely to be smaller than 0.24 $\mathrm{M}_{\odot}$. Constraints on the dust production and mass-loss are now becoming available for giants belonging to other GCs (Boyer et al. 2009; McDonald et al. 2009, 2011c, and the survey by Origlia et al.), and will eventually provide a complete investigation of the differential mass-loss among clusters with different metallicities and HB morphologies.

Asteroseismology promises to shed new light on this problem by directly measuring the masses of giant stars in open clusters. The NASA *Kepler* mission, which was launched successfully in 2009 March, includes in its field of view two old open clusters, NGC 6791 and 6819. In these clusters, solar-like oscillations were detected in about 100 giants (see Stello et al. 2010; Basu et al. 2011; Hekker et al. 2011, and Fig. 1), providing independent constraints on the masses and radii of stars on the RGB, as well as on the distance to the clusters and their ages (Basu et al. 2011).

The goal of this paper is to constrain the RGB mass-loss by comparing the average mass of stars in the red clump (RC) with the low-luminosity portion of the RGB [i.e. with $L \lesssim L(\mathrm{RC})$]. The structure of the paper is as follows. In Section 2, we describe the procedures used to estimate the masses of stars from the available seismic and non-seismic constraints. We then address the specific case of NGC 6791 in Section 3, and of NGC 6819 in Section 4. A first comparison with model predictions is presented in Section 5, while a brief summary and future prospects are given in Section 6.

2 ESTIMATING STELLAR MASSES

To estimate stellar masses, we use the average seismic parameters that characterize solar-like oscillation spectra: the so-called average large frequency separation ($\Delta\nu$) and the frequency corresponding to the maximum observed oscillation power ($\nu_{\rm max}$). The large frequency spacing is expected to scale as the square root of the mean density of the star:

$$\Delta\nu \simeq \sqrt{\frac{M/\mathrm{M}_{\odot}}{(R/\mathrm{R}_{\odot})^3}}\,\Delta\nu_{\odot}, \qquad (1)$$

where $\Delta\nu_{\odot} = 135\,\mu$Hz. The frequency of maximum power is approximatively proportional to the acoustic cut-off frequency (Brown

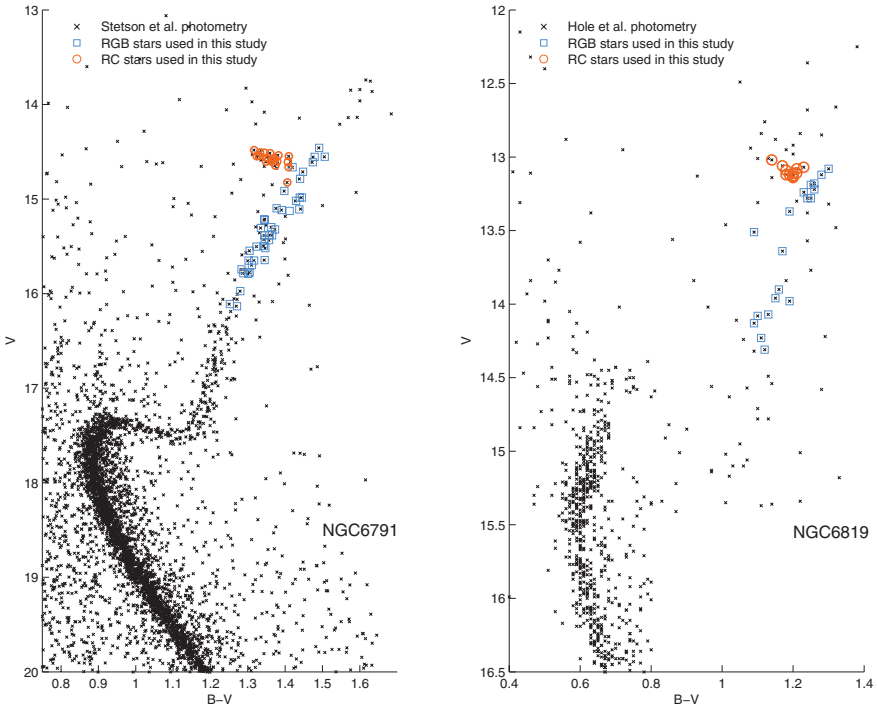

Figure 1. CMD of NGC 6791 (left-hand panel) and NGC 6819 (right-hand panel). Photometric data are taken from Stetson, Bruntt & Grundahl (2003) and Hole et al. (2009), respectively. RGB stars used in this work are marked by open squares and RC stars by open circles. See Section 3.2 for a description of the target selection.

et al. 1991; Kjeldsen & Bedding 1995; Mosser et al. 2010; Belkacem et al. 2011), and therefore

$$\nu_{\rm max} \simeq \frac{M/{\rm M}_\odot}{(R/{\rm R}_\odot)^2\sqrt{T_{\rm eff}/T_{\rm eff,\odot}}}\nu_{\rm max,\odot}\,, \tag{2}$$

where $\nu_{\rm max,\odot} = 3100\,\mu$Hz and $T_{\rm eff,\odot} = 5777$ K.

These scaling relations are widely used to estimate masses and radii of red giants (see e.g. Stello et al. 2008; Kallinger et al. 2010; Mosser et al. 2010), but they are based on simplifying assumptions that remain to be independently verified. Recent advances have been made on providing a theoretical basis for the relation between the acoustic cut-off frequency and $\nu_{\rm max}$ (Belkacem et al. 2011), and preliminary investigations with stellar models (Stello et al. 2009) indicate that the scaling relations hold to within ∼3 per cent on the main sequence and RGB (see also White et al. 2011).

Depending on the observational constraints available, we may derive mass estimates from equations (1) and (2) alone, or via their combination with other available information from non-seismic observations. When no information on distance/luminosity is available, which is usually the case for field stars, equations (1) and (2) may be solved to derive M and R (see e.g. Kallinger et al. 2010; Mosser et al. 2010):

$$\frac{M}{{\rm M}_\odot} \simeq \left(\frac{\nu_{\rm max}}{\nu_{\rm max,\odot}}\right)^3 \left(\frac{\Delta\nu}{\Delta\nu_\odot}\right)^{-4} \left(\frac{T_{\rm eff}}{T_{\rm eff,\odot}}\right)^{3/2}, \tag{3}$$

$$\frac{R}{{\rm R}_\odot} \simeq \left(\frac{\nu_{\rm max}}{\nu_{\rm max,\odot}}\right) \left(\frac{\Delta\nu}{\Delta\nu_\odot}\right)^{-2} \left(\frac{T_{\rm eff}}{T_{\rm eff,\odot}}\right)^{1/2}. \tag{4}$$

In the case of clusters, we can use the distance/luminosities estimated with independent methods (i.e. via isochrone fitting or eclipsing binaries) as an additional constraint. Including this information allows M to be estimated also from equation (1) or equation (2) alone (see equations 5 and 6, respectively), or in combination leading to a mass estimate with no explicit dependence on $T_{\rm eff}$ (as in equation 7):

$$\frac{M}{{\rm M}_\odot} \simeq \left(\frac{\Delta\nu}{\Delta\nu_\odot}\right)^2 \left(\frac{L}{{\rm L}_\odot}\right)^{3/2} \left(\frac{T_{\rm eff}}{T_{\rm eff,\odot}}\right)^{-6}, \tag{5}$$

$$\frac{M}{{\rm M}_\odot} \simeq \left(\frac{\nu_{\rm max}}{\nu_{\rm max,\odot}}\right) \left(\frac{L}{{\rm L}_\odot}\right) \left(\frac{T_{\rm eff}}{T_{\rm eff,\odot}}\right)^{-7/2}, \tag{6}$$

$$\frac{M}{{\rm M}_\odot} \simeq \left(\frac{\nu_{\rm max}}{\nu_{\rm max,\odot}}\right)^{12/5} \left(\frac{\Delta\nu}{\Delta\nu_\odot}\right)^{-14/5} \left(\frac{L}{{\rm L}_\odot}\right)^{3/10}. \tag{7}$$

In the following sections, we use equations (3)–(7) directly to estimate M (and R) without adding any extra dependence on stellar models. As illustrated in detail e.g. by Gai et al. (2011), additional (so-called 'grid-based') methods to estimate M and R can be designed. These procedures are also based on equations (1) and (2) but, by searching solutions for M and R in grids of evolutionary tracks, have the advantage of reducing uncertainties on the derived mass and radius, at the price of some model dependence that we prefer to avoid in this study.

2.1 Error estimates

The formal uncertainties (σ_i) on the masses (M_i) of the stars were used to compute a weighted average mass for stars belonging to the RGB and for stars in the RC:

$$\overline{M} = \frac{\sum_1^N M_i/\sigma_i^2}{\sum_1^N 1/\sigma_i^2}.$$

The uncertainties in these averages were estimated from the weighted scatter in the masses, i.e.

$$\sigma_{\overline{M}} = t[N-1]\sqrt{\frac{\sum_1^N \frac{\left(M_i-\overline{M}\right)^2}{\sigma_i^2}}{(N-1)\sum_1^N 1/\sigma_i^2}}.$$

Due to the small number of stars in the samples, the correction factor $t[N-1]$ was drawn from the Student's t-distribution with $N-1$ degrees of freedom in order to assess the confidence limits correctly (see e.g. Chaplin et al. 1998). We adopted 68 per cent as the 1σ confidence level.

To assess how well the formal fitting uncertainties reflected the scatter in the data, we computed the ratio $z = \sigma_{\overline{M}}/\overline{\sigma_M}$, where $\overline{\sigma_M}$ is the weighted mean uncertainty estimated from the formal uncertainties on the masses, i.e.

$$\overline{\sigma_M} = \left(\sum_1^N 1/\sigma_i^2\right)^{-1/2}.$$

If mass scatter is dominated by random errors and the formal uncertainties reflect the true observational uncertainties, then $z \sim 1$.

The uncertainty on $\Delta\overline{M} = \overline{M}_{\rm RGB} - \overline{M}_{\rm RC}$ due to random errors was finally computed as

$$\sigma_{\Delta\overline{M}} = \sqrt{\sigma^2_{\overline{M}_{\rm RGB}} + \sigma^2_{\overline{M}_{\rm RC}}}.$$

3 NGC 6791

NGC 6791 is an old open cluster, with age estimates ranging from ∼7 to ∼12 Gyr, depending on the choice of reddening and metallicity (see Chaboyer, Green & Liebert 1999; Stetson et al. 2003). More recent studies (Basu et al. 2011; Brogaard et al. 2011) point towards the lower end of this age interval. This cluster has a solar [α/Fe] ratio (Origlia et al. 2006) and is one of the most metal-rich clusters in our Galaxy (Friel & Janes 1993) with a metallicity of [Fe/H] = + 0.3 to + 0.5 (e.g. Origlia et al. 2006; Brogaard et al. 2011, and references therein).

3.1 Mass-loss in NGC 6791: a puzzling open question

As summarized in the following paragraphs, an issue widely debated in the literature is whether the high metallicity of NGC 6791 may lead to higher-than-average mass-loss rates along the RGB, and whether such enhanced mass-loss could explain the very peculiar luminosity distribution of its white dwarfs.

By examining the white dwarf data in the deep *Hubble Space Telescope* photometry analysed by King et al. (2005), Bedin et al. (2005) found a rich population of hundreds of white dwarfs. Surprisingly, the luminosity function of these stars showed two peaks, the dimmer one possibly consistent with the 'normal turn-off age of ∼8 Gyr (but see below), the brighter one indicating a much younger age of ∼2.4 Gyr. White dwarf dating of open clusters and GC has often been used in the literature, and generally provides results consistent with the turn-off dating (von Hippel 2005; Hansen et al. 2007). For NGC 6791, Hansen (2005) speculated that the peculiar luminosity function could be related to high rates of mass-loss. If all the cluster stars formed at the same epoch (∼8 Gyr ago), and if there has been significant mass-loss on the RGB, many stars may have been reduced to a mass below the threshold to ignite the core helium flash. They would evolve much more slowly than the normal carbon–oxygen white dwarfs in the cluster, leading to a more luminous peak in the white dwarf luminosity function. This explanation proposed by Hansen (2005) received support from Kalirai et al. (2007), who derived a very low average mass ($M \sim 0.43 \pm 0.06\,{\rm M}_\odot$) for the luminous white dwarfs for which they obtained Keck/LRIS spectra, well below the limit for helium ignition in a degenerate core. In addition, the post-helium flash, helium-core-burning stars in this cluster are divided into a red giant clump and an extremely blue HB (e.g. Kalirai et al. 2007). The latter may be populated by the less massive stars evolving from the RGB that were still able to ignite a late helium core flash (e.g. Castellani & Castellani 1993; Brown et al. 2001). Stars with slightly higher mass-loss do not ignite helium and evolved directly into helium white dwarfs, giving rise to the more luminous peak in the white dwarf luminosity function. Since the mass at the turn-off of NGC 6791 is ∼1.1 $\rm M_\odot$ (Brogaard et al. 2011), a huge mass-loss, possibly connected to the high metallicity of the cluster, must have occurred if the above scenario is true.

This tentative explanation was disputed by van Loon, Boyer & McDonald (2008), who found that the RGB luminosity function does not show any signs of star depletion, and that the number of HB (clump) stars is consistent with most cluster stars evolving through the helium flash. In addition, dust – a sign of extreme mass-loss – was not detected around the most luminous giants. More recently, Bedin et al. (2008a) used additional data to examine the white dwarf sequence in NGC 6791, confirming a second dimmer peak in the luminosity function. Since the first peak is ∼0.75 mag brighter than the dimmer one, Bedin et al. (2008b) proposed that binary white dwarfs are responsible for the brighter peak. This explanation required that more than ∼30 per cent of the white dwarfs are binaries. In this context, the extreme HB (EHB) can be attributed to binary evolution following the same scenario as the production of extreme B and O subdwarfs in the Galactic field (e.g. Han et al. 2003).

In the new data analysed by Bedin et al. (2008b), a helium white dwarf population does not seem to agree with the colour distribution of the cooling sequences, while a further problem emerged for the interpretation of the dimmer peak, in that its cooling age is ∼6 Gyr, compared with the ∼8 Gyr turn-off age. This latter problem has been recently addressed by including in the modelling the energy released by the sedimentation of ^{22}Ne and of the C–O mixture in the white dwarf core (Deloye & Bildsten 2002; Althaus et al. 2010; García-Berro et al. 2010), which has the effect of lengthening the evolution of the C–O white dwarfs. The recent analysis by García-Berro et al. (2011) also favours a significant population of unresolved binaries as the most likely explanation for the observed white dwarf luminosity function.

3.2 Targets and data

For our initial set of targets, we took the stars listed by Stello et al. (2011a), but removed those listed as seismic non-members and blended stars. To avoid possible contamination by AGB stars, we then removed stars with $L > L$(RC), and subsequently separated the remaining stars into two groups, RGB and RC stars, by visual inspection of the colour–magnitude diagram (CMD). This classification agrees with the one presented by Stello et al. (2011a, table 1). Recent work by Montalbán et al. (2010), Bedding et al. (2011) and Mosser et al. (2011) has shown that the characteristics of the $\ell = 1$ ridge in the echelle diagram can be used as an indicator of evolutionary state of low-mass giants. A detailed and systematic analysis of the properties of $\ell = 1$ modes in cluster stars is beyond the scope of this paper. None the less, by visual inspection of echelle

diagrams, we could identify two misclassified stars by looking at the typical spacing between $\ell = 1$ modes (see examples in Bedding et al. 2011). The first one is KIC 2437103, which we now identify as a core-He-burning star, and the second one is KIC 2437589 which has a spectrum not compatible with a RC star and deserves further analysis. After this selection, we are left with 40 stars on the RGB and 19 stars in the RC (see Fig. 1).

If the mass-loss is very high, then the helium-burning stars that lost the most mass will not be in the RC, but rather on the corresponding flat part of the HB at higher $T_{\rm eff}$ and lower L. Since our sample only includes RC stars, one might suspect that this introduces a selection bias. However, as shown in the membership study by Platais et al. (2011), there are only 12 potential low-mass helium-burning stars outside the RC (disregarding the EHB stars, which most likely result from binary evolution). Among these, many are likely to be blue stragglers or non-members (see their fig. 1 and table 1). Furthermore, work in progress (Brogaard et al., in preparation) shows that a theoretical zero-age HB (ZAHB) that matches the RC stars is brighter than the potential low-mass HB stars. It also shows that the bluest of these [star 2–17, first analysed by Peterson & Green (1998) and often associated with the HB] is actually a blue straggler. Based on this, we believe that there are no, or at most a couple, helium-burning stars present with masses smaller than those in the RC.

The photometric time series data were obtained by the *Kepler* space telescope (Koch et al. 2010) between 2009 May 12 and 2010 March 20, known as observing quarters 1–4. We used the 'long cadence' observing mode ($\Delta t = 29.4$ min; Jenkins et al. 2010b), which provided about 14 000 data points per star. The data reduction from raw images to the final light curves is described by Jenkins et al. (2010a), García et al. (2011) and Stello et al. (2011a). A detailed description of the asteroseismic parameters used in this work is given by Stello et al. (2011b), who used the method of Huber et al. (2009) to measure $\Delta\nu$ and $\nu_{\rm max}$. The average uncertainties in $\Delta\nu$ and $\nu_{\rm max}$ in this sample of targets are 1.3 and 1.7 per cent, respectively. Other analyses of the same cluster are given in our companion papers: Basu et al. (2011), Hekker et al. (2011) and Stello et al. (2011b).

The effective temperatures used in this study are, following Basu et al. (2011), Hekker et al. (2011), Stello et al. (2011a) and Stello et al. (2011b), based on the $(V - K)$ colour and on the calibrations of Ramírez & Meléndez (2005). The value we adopted for the reddening is $E(B - V) = 0.16 \pm 0.02$ mag (Brogaard et al. 2011) and for the metallicity [Fe/H] $= +0.3$. As presented by Hekker et al. (2011), the estimated random star-to-star error on $T_{\rm eff}$ is about 50 K, which we also adopt in the following analysis. However, systematic errors on the $T_{\rm eff}$ scale due to colour–temperature calibrations and reddening could increase the error budget up to $\sim$110 K (Hekker et al. 2011); we discuss in Section 3.4 the effect of systematic errors in $T_{\rm eff}$ on our results.

Finally, luminosities were derived using V magnitudes from Stetson et al. (2003), the bolometric corrections (BC) by Flower (1996) and the distance modulus $(m - M)_V = 13.51 \pm 0.06$ mag estimated by Brogaard et al. (2011) using eclipsing binaries.

3.3 Results

We first applied equation (3) to derive masses of stars in our sample from $\nu_{\rm max}$, $\Delta\nu$ and $T_{\rm eff}$. As presented in the top row of Table 1, we find $\overline{M}_{\rm RGB} = 1.23 \pm 0.02\,{\rm M}_\odot$ and $\overline{M}_{\rm RC} = 1.03 \pm 0.03\,{\rm M}_\odot$. The mass difference we obtain is thus $\Delta\overline{M} = 0.19 \pm 0.04\,{\rm M}_\odot$.

The value of $z = 1.8$–1.9 reported in the first row of Table 1 suggests that the scatter in the population is larger than expected from the formal uncertainties in the masses. This could indicate that uncertainties in the observed quantities are underestimated, provided, of course, that there is no significant intrinsic mass spread within the groups of RGB and RC stars. The derived masses for RGB and RC stars are shown as a function of apparent V magnitude in the top row of Fig. 2.

To check the robustness of the mass determination, we also estimated masses using equations (5), (6) and (7), thereby including independent information on the distance to the cluster (see Section 3.2). The results are presented in Table 1, where we consider separately the contributions from random uncertainties and (in parentheses) systematic errors from the distance. We note that the systematic uncertainty has little impact on $\Delta\overline{M}$ ($\leq$0.01 ${\rm M}_\odot$). The correlation between $T_{\rm eff}$ and BC has been taken into account in the error estimates.

If we consider only RGB stars, excellent agreement is found between $\overline{M}_{\rm RGB}$ derived using different observables and scaling relations (see also Fig. 2, left-hand panels). On the other hand, significant disagreement is found between $\overline{M}_{\rm RC}$ determined with different combinations of scaling relations. As an additional test, and to investigate the reason for this discrepancy, we compared radii determined from L and $T_{\rm eff}$ ($R_{\rm CMD}$) with those derived seismically through equation (4) ($R_{\rm seismo}$). As shown in Fig. 3, for RGB stars, the two determinations of radii agree within 5 per cent [with an average relative difference $(R_{\rm CMD} - R_{\rm seismo})/R_{\rm CMD} = -0.15$ per cent]. This comparison can also be carried out in terms of distance moduli, instead of radii. By coupling photometric constraints with $R_{\rm seismo}$ of the RGB stars, we find an average distance modulus $(m - M)_V = 13.51 \pm 0.02$ mag, where the quoted uncertainty represents only the standard deviation from the mean. This determination is in excellent agreement with the value found by Brogaard et al. (2011) using eclipsing binaries [$(m - M)_V = 13.51 \pm 0.06$; see Section 3.2]. The situation is different for RC stars, whose radii obtained from

Table 1. NGC 6791: average mass of stars in the RGB and RC estimated using different observational constraints and scaling relations (equations 3, 5, 6 and 7). The systematic error on $\overline{M}$ due to the uncertainty on the distance is reported in brackets. z (see Section 2.1) was computed taking into account only random errors in the observables and the correlation between BC and $T_{\rm eff}$. No correction to the $\Delta\nu$ scaling was applied to clump stars.

Equation	$\overline{M}_{\rm RGB} \pm \sigma_{\overline{M}}$	$z_{\rm RGB}$	$\overline{M}_{\rm RC} \pm \sigma_{\overline{M}}$	$z_{\rm RC}$	$\Delta\overline{M} \pm \sigma_{\Delta\overline{M}}$
(3)	1.23 ± 0.02	1.8	1.03 ± 0.03	1.9	0.19 ± 0.04
(5)	$1.22 \pm 0.01\,(0.10)$	0.7	$1.20 \pm 0.02\,(0.10)$	0.6	$0.02 \pm 0.02\,(0.01)$
(6)	$1.23 \pm 0.01\,(0.07)$	1.1	$1.14 \pm 0.02\,(0.06)$	1.1	$0.09 \pm 0.02\,(<0.01)$
(7)	$1.23 \pm 0.02\,(0.02)$	1.9	$1.07 \pm 0.03\,(0.02)$	2.0	$0.16 \pm 0.03\,(<0.01)$

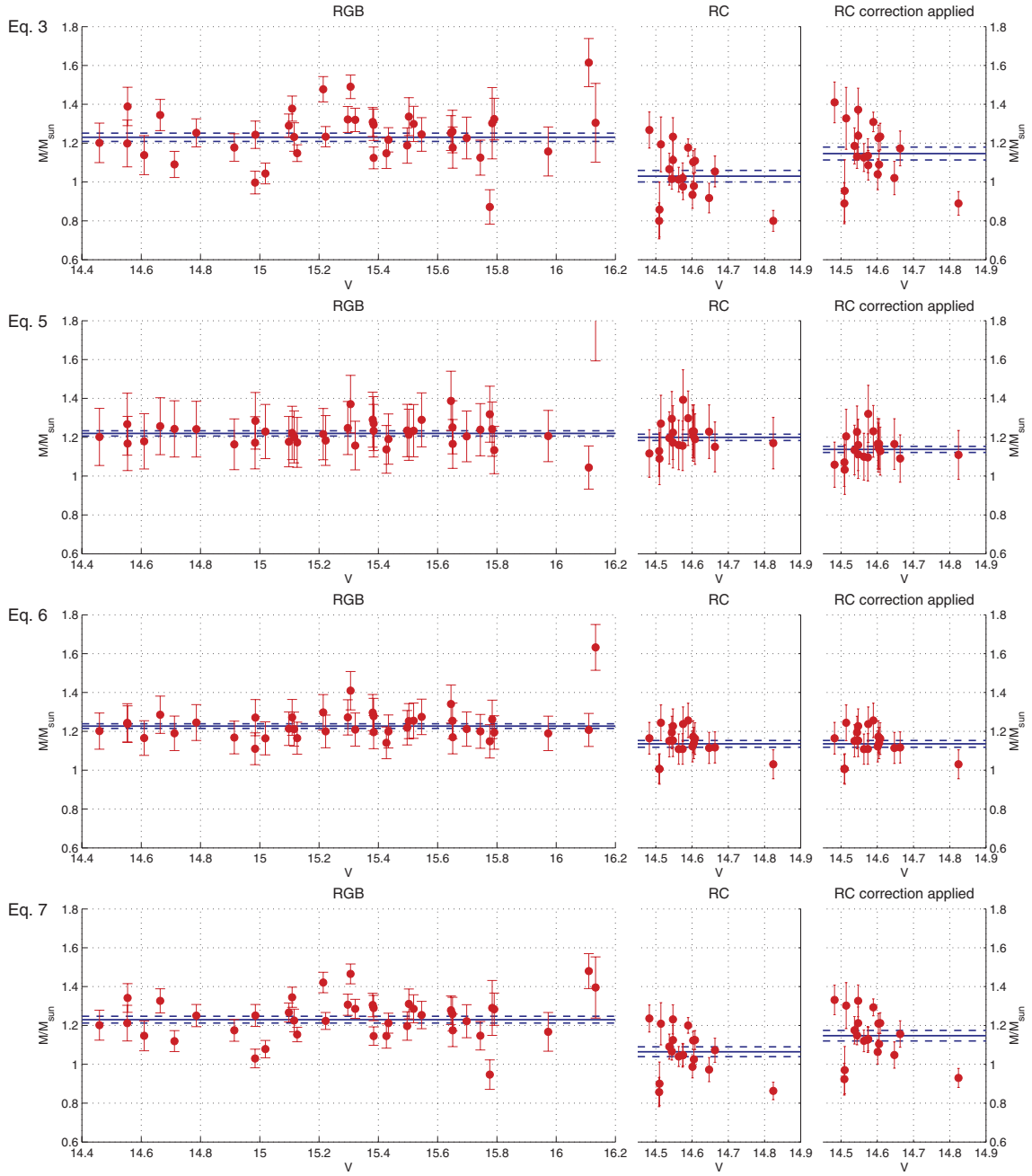

Figure 2. Mass of red giants in NGC 6791 as a function of visual magnitude in the RGB (left-hand panels) and in the RC (central panels). Random errors on the mass estimate of each star are represented by vertical error bars. The average mass of RGB and RC stars is represented with full lines, and the 1σ error bars with dashed lines. Right-hand panels show the masses of RC stars after a correction to the $\Delta\nu$ scaling is applied (see Section 3.4).

equation (4) are systematically smaller than those derived from the CMD, with an average relative difference of -5 per cent. This discrepancy could indicate a systematic error in the scaling relations for RC stars.

3.4 The $\Delta\nu$ scaling relation for RC and RGB stars

Following the asymptotic approximation for acoustic oscillation modes, $\Delta\nu$ is directly related to the sound traveltime in the stellar interior. We therefore expect $\Delta\nu$ to depend on the stellar structure. Given that stars on the RGB have an internal temperature (hence sound speed) distribution significantly different from that of RC stars, we investigated whether this difference could have an impact on the mass determination via the $\Delta\nu$ scaling relation.

We used the code ATON (Ventura, D'Antona & Mazzitelli 2008) to compute stellar models representative of red giants in NGC 6791, i.e. 1.2 $M_{\odot}$ models with initial heavy-element mass fraction $Z = 0.04$, and initial helium mass fraction $Y = 0.30$ (see Montalbán et al. 2010, for more details on the models). The evolution of the models was followed through the helium flash. We then considered two models with the same radius (within 0.1 per cent): one on the RGB and the other in the RC. We computed radial oscillation frequencies with the LOSC code (Scuflaire et al. 2008) and found that the RC model had a mean large frequency separation

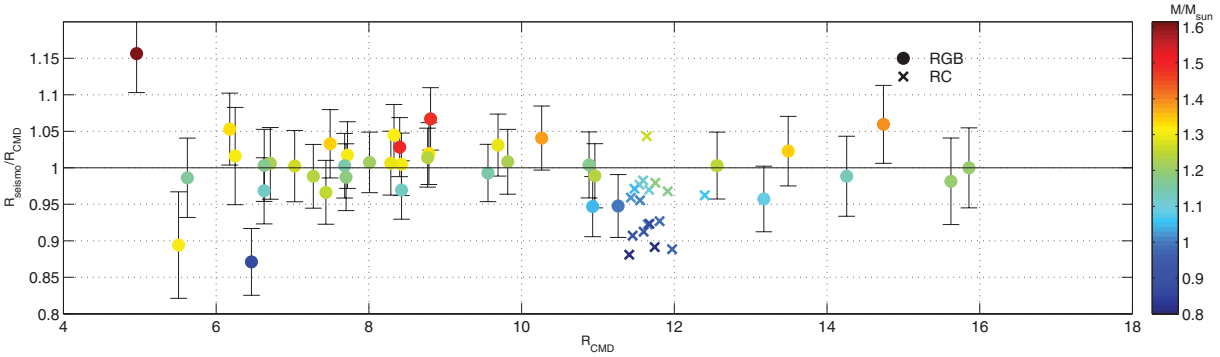

Figure 3. NGC 6791: ratio between radii determined using L and $T_{\rm eff}$ ($R_{\rm CMD}$), and those obtained via equation (4) ($R_{\rm seismo}$). The mass of each star determined via equation (3) is colour coded.

~3.3 per cent larger than the RGB model, despite having the same mean density.

The average large frequency separation is known to be directly related to the behaviour of the sound speed in the stellar interior, since $\Delta\nu \simeq 1/(2\,T_{\rm ac})$, where $T_{\rm ac}$ is the total acoustic radius of the star. The latter is defined as $T_{\rm ac} = t_{\rm ac}(R)$, with $t_{\rm ac}(r) = \int_0^r {\rm d}r'/c(r')$ being the acoustic radius, c the sound speed and R the photospheric radius.

The upper-left panel of Fig. 4 shows the layers contributing to the difference in the overall acoustic radius. As shown in the upper-right panel, the sound speed in the RC model is on average higher (at a given fractional radius) than that of the RGB model, the main reason being the different temperature profile in the two models (lower-right panel). The difference in acoustic radius becomes significant in regions as deep as $m/{\rm M}_\odot \simeq 0.25$, which is where the boundary of the helium core in the RGB model is located (lower-left panel). Finally, we note that while the largest contribution to the overall difference originates in the deep interior, near-surface regions ($r/R \gtrsim 0.9$) also contribute (by 0.8 per cent) to the total 3.5 per cent difference in $T_{\rm ac}$ (upper-left panel of Fig. 4).

These findings suggest that, if we intend to use the $\Delta\nu$ scaling to estimate stellar mean density, a relative correction has to be considered when dealing with RC and RGB stars. This relative correction is expected to be mass-dependent and to be larger for low-mass stars, which have significantly different internal structure when ascending the RGB compared to when they are in the core-He-burning phase. Deriving an accurate theoretical correction of the $\Delta\nu$ scaling, however, is beyond the scope of this paper, as additional models should be considered and detailed tests should be made of the internal structure of such stars. Guided by the representative modelling presented here, we instead adopted an empirical approach to correct the $\Delta\nu$ scaling.

We determined the correction factor to the large frequency separation by minimizing the average relative difference $(R_{\rm CMD} - R_{\rm seismo})/R_{\rm CMD}$ for RC stars. The correction factor derived following this procedure is 2.7 per cent, in good agreement with the correction suggested by the models. Correcting the $\Delta\nu$ scaling for RC stars has a direct effect on $\overline{M}_{\rm RC}$ obtained with different scaling relations. After we applied the correction to the $\Delta\nu$ scaling, the revised average mass of RC stars computed with equations (3), (5) and (7)

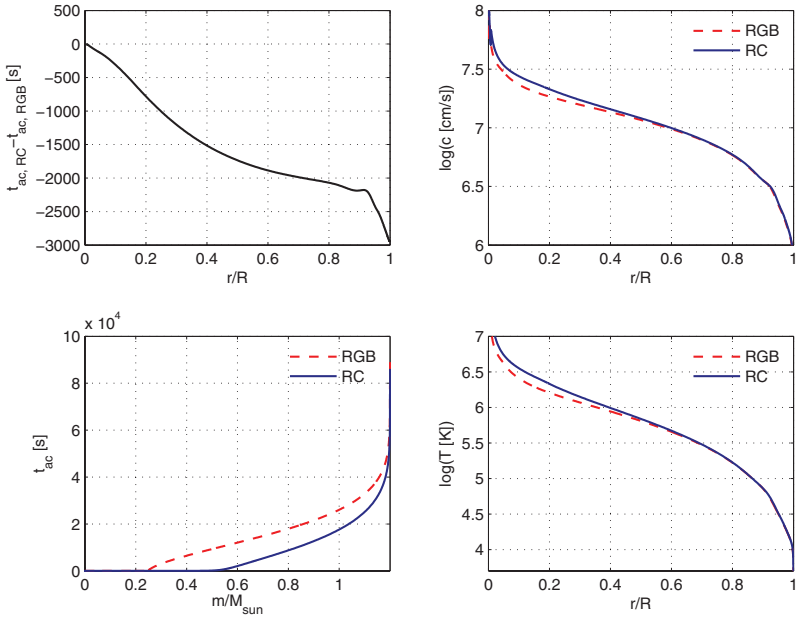

Figure 4. Upper-left panel: difference between the acoustic radius of RGB and RC models of same mass and radius as a function of relative radius. Right-hand panels: sound speed and temperature stratification as a function of the normalized radius in the RGB model (red dashed line) and RC model (blue solid line). Lower-left panel: acoustic radius as a function of mass (in solar units) for the RGB and RC models.

Table 2. As in Table 1, after applying the 2.7 per cent suggested correction to the $\Delta\nu$ scaling for clump stars (see Section 3.4).

Equation	$\overline{M}_{\rm RC} \pm \sigma_{\overline{M}}$	$z_{\rm RC}$	$\Delta\overline{M} \pm \sigma_{\Delta\overline{M}}$
(3)	1.15 ± 0.03	1.8	0.08 ± 0.04
(5)	$1.14 \pm 0.02\,(0.09)$	0.6	$0.08 \pm 0.02\,(0.01)$
(6)	$1.14 \pm 0.02\,(0.06)$	1.1	$0.09 \pm 0.02\,(<0.01)$
(7)	$1.15 \pm 0.03\,(0.02)$	2.0	$0.08 \pm 0.03\,(<0.01)$

agreed within 1σ with the value obtained with equation (6), which does not contain $\Delta\nu$ (see Table 2).

We note that the uncertainties in $R_{\rm seismo}$ and $R_{\rm CMD}$ imply an uncertainty of 1 per cent in the correction factor to the $\Delta\nu$ scaling relation. This leads to an additional source of systematic uncertainty in the mass estimate, which is largest ($0.03\,{\rm M}_{\odot}$) when using equation (3) to determine $\Delta\overline{M}$, and zero when using equation (6). Considering also potential differential temperature scale shifts between the RC and RGB (at the level of 1 per cent), we adopted $0.04\,{\rm M}_{\odot}$ as a conservative estimate of the additional systematic uncertainty in $\Delta\overline{M}$. Taking into account the uncertainties and scatter of the average mass of RC and RGB stars obtained with different scaling relations, we derived our best estimate of the difference between average masses of RGB and RC stars: $\Delta\overline{M} = 0.09 \pm 0.03$ (random) $\pm\, 0.04$ (systematic).

Finally, to check for additional sources of bias due to the $T_{\rm eff}$ scale, we considered effective temperatures determined from $(V - I)$ colours. These $T_{\rm eff}$ introduce small but systematic trends in the derived quantities (e.g. mass versus apparent magnitude) and worsen the agreement between masses and radii derived using different observational constraints. We find, none the less, that $\Delta\overline{M}$ obtained with the different temperature scales agree within the quoted uncertainty range.

4 NGC 6819

NGC 6819 is an open cluster of near-solar metallicity (Bragaglia et al. 2001) estimated to be 2–2.5 Gyr old (Kalirai & Tosi 2004; Basu et al. 2011). Given that the cluster is significantly younger than NGC 6791, a smaller RGB mass-loss is expected. As for the case of NGC 6791, we refer to Basu et al. (2011), Hekker et al. (2011), Stello et al. (2011a) and Stello et al. (2011b) for a description of the asteroseismic data available for the stars in this cluster.

We selected targets on the RGB and in the RC following the same criteria used in Section 3.2, and retained in the final list 19 RGB stars and 13 RC stars. As for NGC 6791, we adopted the effective temperatures determined using $(V - K)$ colours, the colour–temperature calibration of Ramírez & Meléndez (2005) and assuming a reddening $E(B - V) = 0.15$ mag (see Basu et al. 2011) and [Fe/H] = 0.

We then performed a similar analysis as for NGC 6791. However, since no accurate determination of the distance modulus was available for this cluster, we proceeded as in Basu et al. (2011) and estimated the distance modulus using the seismically determined radii of RGB stars and photometric constraints. We found $(m - M)_V = 11.80 \pm 0.02$ mag, where the quoted uncertainty represents only the standard deviation from the mean (see Basu et al. 2011, for a more detailed discussion of systematic uncertainties on the distance determination due to reddening).

We repeated the same steps as in Section 3.3 to determine the average mass of stars on the RGB and in the RC, and present our results in Table 3 and Fig. 5. We note that, as in NGC 6791, $\overline{M}_{\rm RGB}$ is independent of the scaling used, but significant discrepancies appear in the estimated $\overline{M}_{\rm RC}$. Analogously to the case described in Sec 3.4, we used $1.6\,{\rm M}_{\odot}$ stellar models and found that a relative correction to the $\Delta\nu$ scaling was appropriate, and that the radii of RC stars are systematically smaller than those obtained using $T_{\rm eff}$ and L (although we note that L is not an independent quantity, as it is determined using equation 4).

Table 3. NGC 6819: average mass of stars in the RGB and RC estimated using different observational constraints and scaling relations (equations 3, 5, 6 and 7). No correction to the $\Delta\nu$ scaling was applied to clump stars.

Equation	$\overline{M}_{\rm RGB} \pm \sigma_{\overline{M}}$	$z_{\rm RGB}$	$\overline{M}_{\rm RC} \pm \sigma_{\overline{M}}$	$z_{\rm RC}$	$\Delta\overline{M} \pm \sigma_{\Delta\overline{M}}$
(3)	1.61 ± 0.04	2.3	1.52 ± 0.04	2.0	0.09 ± 0.06
(5)	1.61 ± 0.03	0.9	1.70 ± 0.02	0.5	-0.09 ± 0.03
(6)	1.61 ± 0.02	1.4	1.64 ± 0.01	0.6	-0.03 ± 0.03
(7)	1.62 ± 0.03	2.5	1.56 ± 0.03	2.1	0.06 ± 0.04

We found that the correction factor for $\Delta\nu$ that minimizes the relative difference between $R_{\rm CMD}$ and $R_{\rm seismo}$ is 1.9 per cent, which is smaller than for NGC 6791. Again, this is in qualitative agreement with the correction suggested by $1.6\,{\rm M}_{\odot}$ models, as the differences in the sound speed profile between RC and RGB stars of similar luminosity decrease when higher masses are considered (see Table 4).

By combining results from different scaling relations, we derive $\Delta\overline{M} = -0.03 \pm 0.04\,{\rm M}_{\odot}$ for NGC 6819. Due to the lack of an independent and accurate distance measurement, however, we consider this result less robust than the determination of $\Delta\overline{M}$ in NGC 6791.

5 INFERENCES ON THE MASS-LOSS RATE

We now compare the difference between the average mass of low-luminosity RGB and RC stars to theoretical predictions using a revised version of the YZVAR[1] isochrones and stellar evolutionary sequences (Bertelli et al. 2008; Bertelli 2011, private communication). We varied the coefficient η describing the efficiency of the RGB mass-loss rate, which was implemented in the models (see Bertelli et al. 1994) following Reimers (1975a) empirical formulation:

$$\frac{{\rm d}M}{{\rm d}t} = 1.27\,10^{-5}\,\eta\,M^{-1}L^{1.5}\,T_{\rm eff}^{-2}, \qquad (8)$$

where M and L are expressed in solar units, $T_{\rm eff}$ in K and t in yr. A commonly adopted value of the parameter describing the mass-loss efficiency is $\eta = 0.4$ (see e.g. Renzini & Fusi Pecci 1988).

We considered three scenarios: isochrones computed without mass-loss ($\eta = 0$), with moderate mass-loss ($\eta = 0.35$), and with an extreme value of the mass-loss efficiency ($\eta = 0.7$). We note that for these relatively young clusters, such a high mass-loss rate is not enough to suppress the RC and AGB phases, in contrast to old GCs (see e.g. Renzini & Fusi Pecci 1988).

For NGC 6791, we considered a 7-Gyr isochrone, computed with initial helium and heavy-elements mass fractions $Y = 0.30$ and $Z = 0.04$. In the case of NGC 6819, we employed a 2.1-Gyr isochrone with $Y = 0.28$ and $Z = 0.017$. Comparisons between observed and theoretical mass–luminosity diagrams are shown in Fig. 6. In these plots, the masses of individual stars were determined by equation (6), and the luminosities were estimated by combining $T_{\rm eff}$

[1] http://stev.oapd.inaf.it/YZVAR/

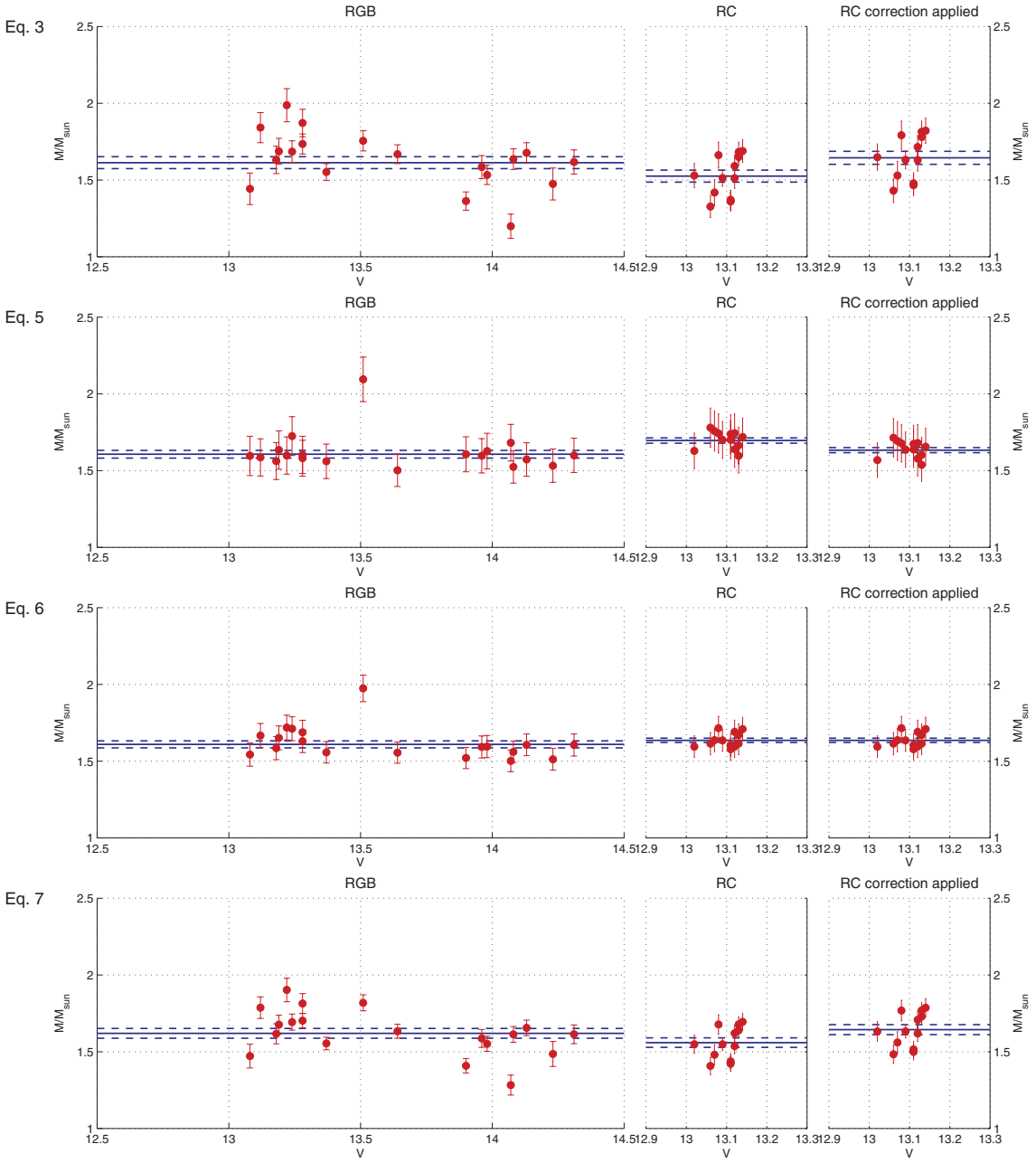

Figure 5. As Fig. 2 but for red giants in NGC 6819.

Table 4. As in Table 3, after applying the 1.9 per cent suggested correction to the $\Delta\nu$ scaling for clump stars.

Equation	$\overline{M}_{\rm RC} \pm \sigma_{\overline{M}}$	$z_{\rm RC}$	$\Delta\overline{M} \pm \sigma_{\Delta\overline{M}}$
(3)	1.65 ± 0.04	2.0	-0.03 ± 0.06
(5)	1.63 ± 0.02	0.5	-0.03 ± 0.03
(6)	1.64 ± 0.01	0.7	-0.03 ± 0.03
(7)	1.64 ± 0.03	2.1	-0.02 ± 0.05

and the photospheric radius obtained via equation (4). The Reimers mass-loss law predicts significant mass-loss only near the RGB tip, hence no appreciable effect is expected ($\Delta M \lesssim 0.01\,{\rm M}_{\odot}$) in the RGB stars we considered, which have relatively low luminosities. With our present measurements, we have no evidence for the time dependence of the mass-loss, as no significant mass gradient is found on the RGB of NGC 6791. Current uncertainties, however, do not allow us to constrain the mass-loss in this portion of the RGB to better than the total mass-loss derived.

The comparison between observed and theoretically expected mass difference between RGB and RC stars is presented in Fig. 7. This first comparison shows that we can exclude very efficient RGB mass-loss and that the data are compatible with mass-loss rates described with a Reimers η parameter smaller than $\sim$0.35 and, in the better constrained case of NGC 6791, higher than 0.1. We note that the relation between $\Delta\overline{M}$ and η predicted by the models has little dependence on the assumed age and chemical composition (e.g. in the case of NGC 6791, we checked the robustness of our main conclusion considering also isochrones of 6 and 9 Gyr, $Y = 0.28, 0.32$ and $Z = 0.025, 0.030$).

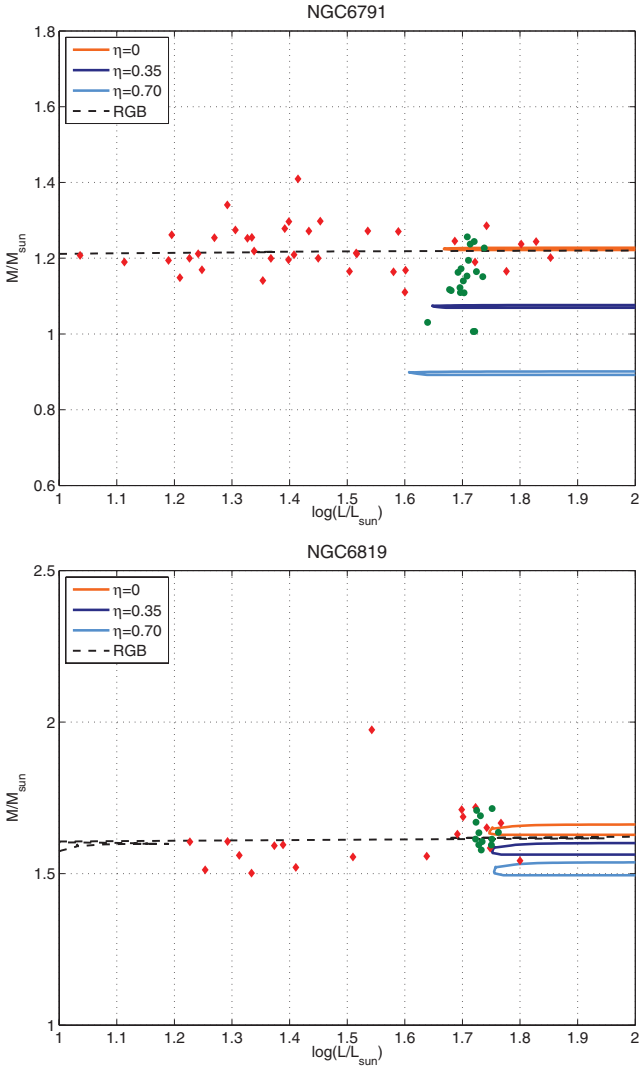

Figure 6. Upper panel: masses of giants in NGC 6791 derived from equation (6) as a function of luminosity. Red and green points indicate RGB and RC stars. Lines represent the 7-Gyr isochrone computed with different mass-loss rates. The RGB part of the isochrone is indicated with a dashed line, while solid lines represent the evolution from the He flash towards the ZAHB, and onwards. Lower panel: same as the upper panel, but for stars in NGC 6819. For this cluster, a 2.1-Gyr, solar-metallicity isochrone was used.

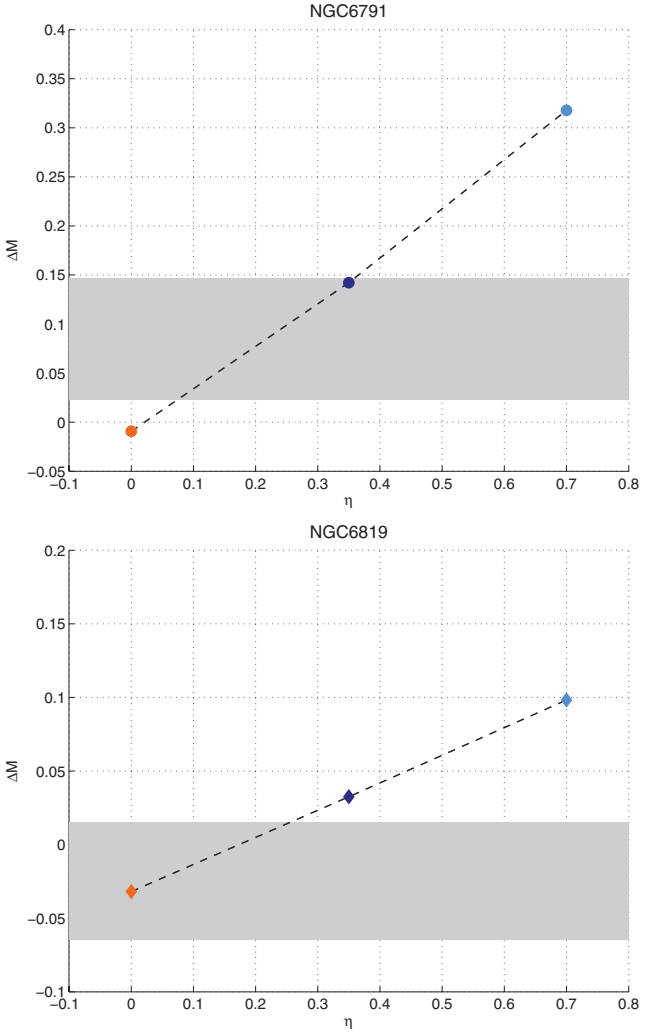

Figure 7. Upper panel: the dots connected by a dashed line shows the difference (ΔM) between the average mass of RGB stars (in the luminosity domain of the targets) and RC stars as a function of the η parameter, resulting from a 7-Gyr model isochrone. The grey areas represent the 1σ region of the observed ΔM. Lower panel: same plot as the upper panel, but for stars in NGC 6819 and a 2.1-Gyr isochrone.

We finally note that in the case of NGC 6819, a negative $\Delta\overline{M}$ is expected from the models with little or no mass-loss. For such a young cluster, $\Delta\overline{M}$ underestimates the integrated mass-loss on the RGB, since the initial mass of stars in the RC is higher than that of stars on the RGB. In the case of the 2.1-Gyr isochrone considered in Figs 6 and 7, the difference in average progenitor mass between RGB and RC stars is $\simeq -0.03\,\mathrm{M}_{\odot}$, hence the observed mass difference is compatible with no mass-loss, as shown in the lower panel of Fig. 7.

6 SUMMARY AND PROSPECTS

We used the average seismic parameters characterizing solar-like oscillations ($\nu_{\rm max}$ and $\Delta\nu$) to estimate the masses of stars in the RC and on the low-luminosity RGB [$L < L$(RC)] of the open clusters NGC 6791 and 6819.

In NGC 6791, $\nu_{\rm max}$ and $\Delta\nu$ were coupled with additional constraints (photometric magnitudes, $T_{\rm eff}$ and distance modulus from eclipsing binaries) to measure stellar radii and to determine the average mass of stars on the RGB and in the RC. When considering RGB stars, we found good agreement between different determinations of radius and mass, while in the RC a larger scatter between $\overline{M}_{\rm RC}$ was found, together with a systematic underestimation of the radii obtained via equation (4) compared to those determined using photometric constraints and the independent distance determination obtained by Brogaard et al. (2011). Supported by a comparison between RC and RGB models, we ascribed this discrepancy to the $\Delta\nu$ scaling (equation 1) and argued that a relative correction of $\sim$3 per cent to $\Delta\nu$ between RC and RGB stars should be adopted for stars in this cluster.

Taking into account the uncertainties in the observational constraints, we found that in NGC 6791 the difference between the average mass of RGB and RC stars is small but significant ($\Delta\overline{M} = 0.09 \pm 0.03$ (random) ± 0.04 (systematic) $\mathrm{M}_{\odot}$). In the context of the controversial and highly debated results on the

mass-loss rates in NGC 6791 (see Section 3.1), our direct estimate of $\Delta\overline{M}$ is incompatible with an extreme mass-loss for this metal-rich cluster. If we describe the mass-loss rate with Reimers prescription (see equation 8), and assume a 7-Gyr isochrone, we find that the observed $\Delta\overline{M}$ is compatible with a mass-loss efficiency parameter of $0.1 \lesssim \eta \lesssim 0.3$. The low mass-loss of the RC stars, coupled with a RC mass-loss dispersion lower than our measurement errors, provides support for our assumption (see Section 3.2) that either no helium-burning stars exist with masses significantly lower than the measured RC stars or, if they do, they must originate from a very different evolution.

Constraints on the RGB mass-loss set by the analysis of NGC 6819 are less compelling, largely because this cluster is too young to exhibit a significant mass-loss (at least according to Reimers formula). Moreover, no accurate and independent information on the distance was available for this cluster.

In the future, a reliable age determination of the clusters obtained by combining all available constraints will potentially allow detailed tests of different formulations of the RGB mass-loss rate (e.g. Catelan 2000; Schröder & Cuntz 2005, 2007), eventually leading to a better understanding of the physical mechanism responsible for the mass-loss itself. Moreover, as the duration of *Kepler* observations increases, it will soon be possible to study in detail the pulsational properties of stars with luminosities higher than the RC. These targets could provide the link between the stars studied in this paper and the luminous ($L \gtrsim 10^3\,L_\odot$) RGB and AGB giants in which a connection between mass-loss and pulsations has been suggested by several studies in the literature (see e.g. Lebzelter & Wood 2005, and references therein).

In this work, we reached a point where possible systematic biases in the $\Delta\nu$ and $\nu_{\rm max}$ scaling relations may become the largest source of uncertainty in the determination of stellar parameters. As shown in Section 3.4, we have found evidence for systematic differences in the $\Delta\nu$ scaling relation between He-burning and H-shell-burning giants. A more systematic study using a larger set of stellar models is needed to address this issue in detail. In particular, robust model-based corrections to the $\Delta\nu$ scaling relation would allow testing in detail possible systematic errors in the $\nu_{\rm max}$ scaling, hence improving the accuracy of the mass determination.

The frequency of maximum power will in general depend on the dynamical properties of near-surface convective layers and on the complex interaction between oscillation modes and convection. The published relations, however, assume a simple scaling of $\nu_{\rm max}$ with the acoustic cut-off frequency in the atmosphere, and simplifying assumptions about the latter. It is therefore possible that evolutionary-state-dependent corrections may be required for $\nu_{\rm max}$ also. However, the close correspondence between the radius anomalies expected from $\Delta\nu$ effects and those seen in NGC 6791 suggests either that the impact of such corrections is modest or that there is some effective cancellation of terms in the radius scalings. The $\nu_{\rm max}$ scaling should be investigated, but a proper formulation would involve detailed convective modelling which is outside the scope of the current work. One promising approach would be to search for residual differences in stars of known mass and radius once more robust theoretical corrections to $\Delta\nu$ are applied, and there is work in preparation pursuing this avenue of approach.

In this context, pulsating red giants with independent masses and/or radii (e.g. binary members and nearby giants) would allow calibration of the $\Delta\nu$ and $\nu_{\rm max}$ scaling relations, and provide an unprecedented, and potentially very accurate, means of determining stellar parameters.

Additional observational constraints that will improve the precision and accuracy of our conclusions include *Kepler* data that will soon be available for most stars in the clusters. Moreover, the availability in the near future of not only average seismic parameters such as $\nu_{\rm max}$ and $\Delta\nu$, but also of accurate frequencies of individual oscillation modes in red giants, will allow more detailed tests of the scaling relations as well as of the internal structure of these stars. Finally, spectroscopic constraints on $T_{\rm eff}$ will also be of great relevance to check the validity of the adopted $T_{\rm eff}$ scale and to further test the robustness of the agreement we find between global parameters of stars determined using different constraints (asteroseismology, photometry, distance determined using eclipsing binaries).

ACKNOWLEDGMENTS

The authors acknowledge the *Kepler* Science Team and all those who have contributed to making the *Kepler* mission possible. Funding for the *Kepler* Discovery mission is provided by NASA's Science Mission Directorate. AM acknowledges the support of the School of Physics and Astronomy, University of Birmingham. KB acknowledges financial support from the Carlsberg Foundation. DS acknowledges support from the Australian Research Council. WJC and YE acknowledge support from the UK STFC. AMS is supported by the European Union International Reintegration Grant PIRG-GA-2009-247732, the MICINN grant AYA08-1839/ESP, by the ESF EUROCORES Programme EuroGENESIS (MICINN grant EUI2009-04170), by SGR grants of the Generalitat de Catalunya and by the EU-FEDER funds. SH acknowledges financial support from the Netherlands Organization for Scientific Research (NWO). This project has been supported by the 'Lendület' program of the Hungarian Academy of Sciences and the Hungarian OTKA grants K83790 and MB08C 81013. RS thanks the support of the János Bolyai Research Scholarship. The research leading to these results has received funding from the European Community's Seventh Framework Programme (FP7/2007-2013) under grant agreement no. 269194.

REFERENCES

Althaus L. G., García-Berro E., Renedo I., Isern J., Córsico A. H., Rohrmann R. D., 2010, ApJ, 719, 612
Basu S. et al., 2011, ApJ, 729, L10
Bedding T. R. et al., 2011, Nat, 471, 608
Bedin L. R., Salaris M., Piotto G., King I. R., Anderson J., Cassisi S., Momany Y., 2005, ApJ, 624, L45
Bedin L. R., King I. R., Anderson J., Piotto G., Salaris M., Cassisi S., Serenelli A., 2008a, ApJ, 678, 1279
Bedin L. R., Salaris M., Piotto G., Cassisi S., Milone A. P., Anderson J., King I. R., 2008b, ApJ, 679, L29
Belkacem K., Goupil M. J., Dupret M. A., Samadi R., Baudin F., Noels A., Mosser B., 2011, A&A, 530, A142
Bertelli G., Bressan A., Chiosi C., Fagotto F., Nasi E., 1994, A&AS, 106, 275
Bertelli G., Girardi L., Marigo P., Nasi E., 2008, A&A, 484, 815
Bowen G. H., 1988, ApJ, 329, 299
Boyer M. L. et al., 2009, ApJ, 705, 746
Boyer M. L. et al., 2010, ApJ, 711, L99
Bragaglia A. et al., 2001, AJ, 121, 327
Brogaard K., Bruntt H., Grundahl F., Clausen J. V., Frandsen S., Vandenberg D. A., Bedin L. R., 2011, A&A, 525, A2
Brown T. M., Gilliland R. L., Noyes R. W., Ramsey L. W., 1991, ApJ, 368, 599
Brown T. M., Sweigart A. V., Lanz T., Landsman W. B., Hubeny I., 2001, ApJ, 562, 368

Carretta E., Bragaglia A., Gratton R., Lucatello S., 2009, A&A, 505, 139
Castellani M., Castellani V., 1993, ApJ, 407, 649
Catelan M., 2000, ApJ, 531, 826
Catelan M., 2009, Ap&SS, 320, 261
Chaboyer B., Green E. M., Liebert J., 1999, AJ, 117, 1360
Chaplin W. J., Elsworth Y., Isaak G. R., Lines R., McLeod C. P., Miller B. A., New R., 1998, MNRAS, 300, 1077
D'Antona F., Caloi V., 2004, ApJ, 611, 871
D'Antona F., Caloi V., Montalbán J., Ventura P., Gratton R., 2002, A&A, 395, 69
Deloye C. J., Bildsten L., 2002, ApJ, 580, 1077
Flower P. J., 1996, ApJ, 469, 355
Friel E. D., Janes K. A., 1993, A&A, 267, 75
Gai N., Basu S., Chaplin W. J., Elsworth Y., 2011, ApJ, 730, 63
García R. A. et al., 2011, MNRAS, 414, L6
García-Berro E. et al., 2010, Nat, 465, 194
García-Berro E., Torres S., Renedo I., Camacho J., Althaus L. G., Córsico A. H., Salaris M., Isern J., 2011, A&A, 533, 31
Goldberg L., 1979, R. Astron. Soc., 20, 361
Gratton R. G. et al., 2001, A&A, 369, 87
Han Z., Podsiadlowski P., Maxted P. F. L., Marsh T. R., 2003, MNRAS, 341, 669
Hansen B. M. S., 2005, ApJ, 635, 522
Hansen B. M. S. et al., 2007, ApJ, 671, 380
Harper G., 1996, in Pallavicini R., Deupree A. K., eds, ASP Conf. Ser. Vol. 109, Cool Stars; Stellar Systems; and the Sun: 9. Astron. Soc. Pac., San Francisco, p. 481
Hekker S. et al., 2011, A&A, 530, A100
Höfner S., 2009, in Henning T., Grün E., Steinacker J., eds, ASP Conf. Ser. Vol. 414, Cosmic Dust - Near and Far. Astron. Soc. Pac., San Francisco, p. 3
Hole K. T., Geller A. M., Mathieu R. D., Platais I., Meibom S., Latham D. W., 2009, AJ, 138, 159
Huber D., Stello D., Bedding T. R., Chaplin W. J., Arentoft T., Quirion P.-O., Kjeldsen H., 2009, Commun. Asteroseismol., 160, 74
Jenkins J. M. et al., 2010a, ApJ, 713, L87
Jenkins J. M. et al., 2010b, ApJ, 713, L120
Judge P. G., Stencel R. E., 1991, ApJ, 371, 357
Kalirai J. S., Tosi M., 2004, MNRAS, 351, 649
Kalirai J. S., Bergeron P., Hansen B. M. S., Kelson D. D., Reitzel D. B., Rich R. M., Richer H. B., 2007, ApJ, 671, 748
Kalirai J. S., Saul Davis D., Richer H. B., Bergeron P., Catelan M., Hansen B. M. S., Rich R. M., 2009, ApJ, 705, 408
Kallinger T. et al., 2010, A&A, 509, A77
King I. R., Bedin L. R., Piotto G., Cassisi S., Anderson J., 2005, AJ, 130, 626
Kjeldsen H., Bedding T. R., 1995, A&A, 293, 87
Koch D. G. et al., 2010, ApJ, 713, L79
Lafon J. P. J., Berruyer N., 1991, The A&AR, 2, 249
Lebzelter T., Wood P. R., 2005, A&A, 441, 1117
McDonald I., van Loon J. T., Decin L., Boyer M. L., Dupree A. K., Evans A., Gehrz R. D., Woodward C. E., 2009, MNRAS, 394, 831
McDonald I., Boyer M. L., van Loon J. T., Zijlstra A. A., 2011a, ApJ, 730, 71
McDonald I. et al., 2011b, ApJS, 193, 23
McDonald I. et al., 2011c, ArXiv e-prints
Montalbán J., Miglio A., Noels A., Scuflaire R., Ventura P., 2010, ApJ, 721, L182
Mosser B. et al., 2010, A&A, 517, A22
Mosser B. et al., 2011, A&A, 532, A86
Mullan D. J., 1978, ApJ, 226, 151
Origlia L., Ferraro F. R., Fusi Pecci F., Rood R. T., 2002, ApJ, 571, 458
Origlia L., Valenti E., Rich R. M., Ferraro F. R., 2006, ApJ, 646, 499
Origlia L., Rood R. T., Fabbri S., Ferraro F. R., Fusi Pecci F., Rich R. M., 2007, ApJ, 667, L85
Origlia L., Rood R. T., Fabbri S., Ferraro F. R., Fusi Pecci F., Rich R. M., Dalessandro E., 2010, ApJ, 718, 522
Peterson R. C., Green E. M., 1998, ApJ, 502, L39
Piotto G. et al., 2005, ApJ, 621, 777
Piotto G. et al., 2007, ApJ, 661, L53
Platais I., Cudworth K. M., Kozhurina-Platais V., McLaughlin D. E., Meibom S., Veillet C., 2011, ApJ, 733, L1
Ramírez I., Meléndez J., 2005, ApJ, 626, 446
Reimers D., 1975a, Mém. Soc. R. Sci. Liège, 8, 369
Reimers D., 1975b, in Baschek B., Kegel W. H., Traving G., eds, Circumstellar Envelopes and Mass Loss of Red Giant Stars. Springer-Verlag, New York, p. 229
Renzini A., Fusi Pecci F., 1988, ARA&A, 26, 199
Schröder K.-P., Cuntz M., 2005, ApJ, 630, L73
Schröder K.-P., Cuntz M., 2007, A&A, 465, 593
Scuflaire R., Théado S., Montalbán J., Miglio A., Bourge P.-O., Godart M., Thoul A., Noels A., 2008, Ap&SS, 316, 83
Stello D., Bruntt H., Preston H., Buzasi D., 2008, ApJ, 674, L53
Stello D., Chaplin W. J., Basu S., Elsworth Y., Bedding T. R., 2009, MNRAS, 400, L80
Stello D. et al., 2010, ApJ, 713, L182
Stello D. et al., 2011a, ApJ, 737, L10
Stello D. et al., 2011b, ApJ, 739, 13
Stetson P. B., Bruntt H., Grundahl F., 2003, PASP, 115, 413
Sweigart A. V., Gross P. G., 1976, ApJS, 32, 367
van Loon J. T., Boyer M. L., McDonald I., 2008, ApJ, 680, L49
Ventura P., D'Antona F., Mazzitelli I., 2008, Ap&SS, 316, 93
von Hippel T., 2005, ApJ, 622, 565
White T. et al., 2011, ApJ, 742, L3
Wood P. R., 1979, ApJ, 227, 220

This paper has been typeset from a TEX/LATEX file prepared by the author.